Genomic Anatomy of a Premier Major Histocompatibility Complex Paralogous Region on Chromosome 1q21–q22

Takashi Shiina,[1] Asako Ando,[1] Yumiko Suto,[2] Fumio Kasai,[2] Atsuko Shigenari,[1] Nobusada Takishima,[1] Eri Kikkawa,[1] Kyoko Iwata,[1] Yuko Kuwano,[1] Yuka Kitamura,[1] Yumiko Matsuzawa,[1] Kazumi Sano,[1] Masahiro Nogami,[1] Hisako Kawata,[1] Suyun Li,[1] Yasuhito Fukuzumi,[3] Masaaki Yamazaki,[3] Hiroyuki Tashiro,[3] Gen Tamiya,[1] Atsushi Kohda,[4] Katsuzumi Okumura,[4] Toshimichi Ikemura,[5] Eiichi Soeda,[6] Nobuhisa Mizuki,[7] Minoru Kimura,[1] Seiamak Bahram,[8] and Hidetoshi Inoko[1,9]

[1]Department of Genetic Information, Division of Molecular Life Science, Tokai University School of Medicine, Bohseidai, Isehara, Kanagawa 259-1193, Japan; [2]Department of Biological Science, Graduate School of Science, The University of Tokyo, Bunkyo-ku, Tokyo 113-0033, Japan; [3] Bioscience Research Laboratory, Fujiya Co., Ltd., Soya, Hadano, Kanagawa 257-0031, Japan; [4] Faculty of Bioresources, Mie University, Tsu, Mie 514-0008, Japan; [5]Department of Evolutionary Genetics, National Institute of Genetics, Mishima, Shizuoka 411-0801, Japan; [6]Tsu Kuba, Life Science Center, The Institute of Physical and Chemical Research (RIKEN), Yatabe-choh, Tsukuba, Ibaraki 305-0861, Japan; [7]Department of Ophthalmology, Yokohama City University School of Medicine, Kanazawa-ku, Yokohama, Kanagawa 236-0004, Japan; [8]INSERM-CReS, Centre de Recherche d'Immunologie et d'Hématologie, 67085 Strasbourg, France

Human chromosomes 1q21–q25, 6p21.3–22.2, 9q33–q34, and 19p13.1–p13.4 carry clusters of paralogous loci, to date best defined by the flagship 6p MHC region. They have presumably been created by two rounds of large-scale genomic duplications around the time of vertebrate emergence. Phylogenetically, the 1q21–25 region seems most closely related to the 6p21.3 MHC region, as it is only the MHC paralogous region that includes bona fide *MHC* class I genes, the *CD1* and *MR1* loci. Here, to clarify the genomic structure of this model MHC paralogous region as well as to gain insight into the evolutionary dynamics of the entire quadriplication process, a detailed analysis of a critical 1.7 megabase (Mb) region was performed. To this end, a composite, deep, YAC, BAC, and PAC contig encompassing all five *CD1* genes and linking the centromeric +P5 locus to the telomeric *KRTC7* locus was constructed. Within this contig a 1.1-Mb BAC and PAC core segment joining *CD1D* to *FCERIA* was fully sequenced and thoroughly analyzed. This led to the mapping of a total of 41 genes (12 expressed genes, 12 possibly expressed genes, and 17 pseudogenes), among which 31 were novel. The latter include 20 olfactory receptor (*OR*) genes, 9 of which are potentially expressed. Importantly, *CD1*, *SPTA1*, *OR*, and *FCERIA* belong to multigene families, which have paralogues in the other three regions. Furthermore, it is noteworthy that 12 of the 13 expressed genes in the 1q21–q22 region around the *CD1* loci are immunologically relevant. In addition to *CD1A–E*, these include *SPTA1*, *MNDA*, *IFI–16*, *AIM2*, *BL1A*, *FY* and *FCERIA*. This functional convergence of structurally unrelated genes is reminiscent of the 6p MHC region, and perhaps represents the emergence of yet another antigen presentation gene cluster, in this case dedicated to lipid/glycolipid antigens rather than antigen-derived peptides.

[The nucleotide sequence data reported in this paper have been submitted to the DDBJ, EMBL, and GenBank databases under accession nos. AB045357–AB045365.]

The 3.6-Mb human Major Histocompatibility Complex (MHC; also known as the Human leukocyte antigen, HLA) on chromosome 6p21.3 is a critical repository for immune response genes. This 230-gene–rich segment has taught us a great deal about immunity as well as about the evolutionary dynamics of compact genomic segments (Campbell and Trowsdale 1997; The MHC Sequencing Consortium 1999; Shiina et al. 1999). Extensive analysis of the genomic organization of the HLA region has revealed that at least 27 of its resident genes possess duplicated copies in at least one of three other restricted regions on chromosomes 1q21–q25,

[9]Corresponding author.
E-MAIL hinoko@is.icc.u-tokai.ac.jp; FAX 81 463 94 8884.
Article and publication are at www.genome.org/cgi/doi/10.1101/gr.175801.

9q33–q34, and 19p13.1–p13.4 (Sugaya et al. 1994, 1997; Kasahara et al. 1996; Katsanis et al. 1996; Endo et al. 1997; Hughes 1998; Kasahara 1999). ABC transporter gene family members are located on 6p21.3 (*TAP1*, *TAP2*), 1q25 (*EST31252*), and 9q34 (*ABC2*), proteasome β-type subunit loci can be found on 6p21.3 (*LMP2*, *LMP7*) as well as 9q34 (*PSMB7*), pre-B cell leukemia transcription factors are readily identified on 6p21.3 (*PBX2*), 1q23 (*PBX1*), and 9q33–q34 (*PBX3*), and *NOTCH* genes are located on 6p21.3 (*NOTCH4*), 9q34.3 (*NOTCH1*) and 19p13.2–p13.1 (*NOTCH3*). These observations suggest that these four paralogous regions were generated from a common ancestor after two rounds of chromosomal duplication. Moreover, these large-scale duplications possibly enabled at least one of these quadruplicate regions to be relaxed from functional constraints, allowing the formation of the present-day vertebrate MHC, the sophisticated machinery at the heart of the acquired immune system (Abi-Rached et al. 1999). A number of indirect evidences, especially the sequence comparison as well as phylogenetic tree analysis of a number of paralogous genes, allows tracing back these duplicatives events to a common ancestor of jawed vertebrates, from the lineage leading to hagfish and lamprey (Kasahara 1999).

Among the above-mentioned paralogous regions, that of 1q21–q25 is unique because it is the only one outside the MHC carrying divergent, yet genuine histocompatibility-like loci, *CD1* and *MR1* (Albertson et al. 1988; Hashimoto et al. 1995; Riegert et al. 1998). CD1 molecules are cell surface glycoproteins structurally and functionally similar to MHC class I molecules (Calabi and Millstein 1986; Martin et al. 1986). The main difference between these two classes of antigen-presenting loci is indeed their "cargo" peptides in the case of 6p-located MHC class I molecules, and a diverse admixture of glycolipids (issued mainly by various pathogens) in the case of CD1 molecules. This diversification of the presentation capacity of MHC molecules greatly enhances the surveillance capacity of patrolling cytotoxic T cells (Sieling et al. 1995; Burdin et al. 1998). There are five *CD1* genes, *CD1A* to *CD1E*, originally identified within a 190-kb cosmid segment (Calabi and Milstein 1986; Martin et al. 1987; Calabi et al. 1989; Yu and Milstein 1989). Based on sequence divergence, the *CD1* genes can be ordered into three groups: (1) *CD1A*, *CD1B*, and *CD1C*, (2) *CD1D*, and (3) *CD1E* (Hughes 1991). Only homologs of human *CD1D* have been identified in the mouse (Balk et al. 1991), and the rat (Ichimiya et al. 1994). *CD1D* might be a vestige of the ancestral *CD1*, which plausibly created the present-day human *CD1* cluster through sequential duplications (Yu and Mulatein 1989).

Furthermore, paralleling the chromosome 6 HLA region, the CD1 region is of great biomedical importance, as a number of disease-susceptibility loci have been mapped to 1q21–q23; these include genes for elliptocytosis-2, spherocytosis, pyropoikilocytosis (Gallagher et al. 1992), autosomal dominant nonsyndoromic deafness, autosomal dominant nonsyndromic sensorineural 7 (Fagerheim et al. 1996), familial hemiplegic migraine (Ducrons et al. 1997), familial partial lipodystrophy (Jackson et al. 1998), and familial schizophrenia (Brzustowicz et al. 2000). This region has also been implicated in a number of chromosomal translocations; for example t (1; 19) (q23; p13) in lymphoblastic leukemias and t (X; 1) (p11; q21) in papillary renal cell carcinoma (Williams et al. 1984; Weterman et al. 1996).

To clarify the genomic organization of this paralogous CD1 region, and to understand the evolutionary process through which the MHC system acquired its present-day structure, we aimed to establish a comprehensive gene map of a critical 1.7-Mb region. A composite YAC, BAC, and PAC contig was thus constructed, and a core segment of 1.1 Mb encompassing the *CD1* genes was completely sequenced. This 1.7-Mb region was found to contain 10 known genes and 31 newly mapped genes or gene candidates including 20 ORctory receptors.

RESULTS

High-Resolution Mapping of the 1.7-Mb Region between the +P5 Site and *FCERIA* Gene

To clarify the molecular structure and gene organization of a segment of chromosome 1q21–q22 region, paralogous to the MHC and containing the MHC class I-like *CD1* genes, we initially PCR-screened YAC, BAC, and PAC libraries with STS and locus/gene-specific primers. As a result, 33 YACs, 8 BACs, and 51 PACs were isolated and assembled into a contig. Their identity was confirmed by Southern hybridizations with clone-derived PCR and *Eco*RI fragments (data not shown). Below is a description of the cloning and the characterization strategy.

Three YAC clones (800C2, 887G1, and 933H7) containing all of the *CD1* genes were isolated from the CEPH YAC library using *CD1C* primer pairs (Fig. 1) (Walsh et al. 1996). Each *CD1* gene within the clones was identified by PCR using *CD1A-E* locus-specific primer pairs (Table 1). The *CD1D* and *CD1A* genes were included in an additional YAC clone, 367B12. The PAC clone, 810N20, which had a 140-kb insert, contained three *CD1* genes: *CD1D*, *CD1A*, and *CD1C*. The *CD1B* and *CD1E* genes were included in a telomeric overlapping PAC clone, 893N23. As shown in Figure 1, the order of the five *CD1* genes was thus established as *CD1D —CD1A—CD1C—CD1B—CD1E* from centromere to telomere, spanning ~190 kb, in accordance with previous predictions (Yu and Milstein 1989). A PCR primer pair for +P5 (D1S3309E), a target binding

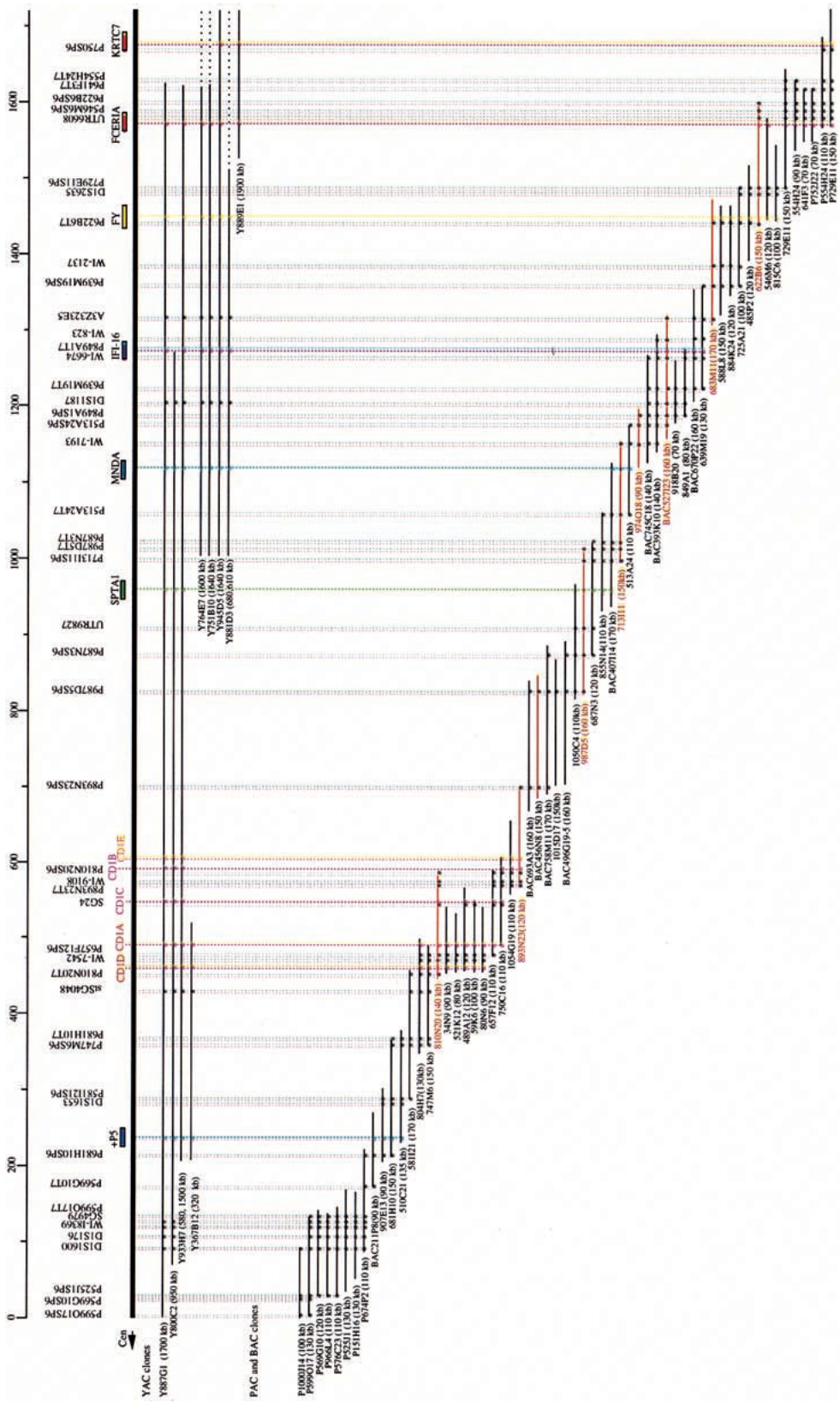

Figure 1 1.7 Mb of a YAC, BAC, and PAC contig between the +P5 and KRTC7 loci. A 1.7-Mb contig constructed by 9 YAC, 8 BAC, and 51 PAC clones is shown with addresses, sizes, markers, and gene contents. BAC and PAC clones subjected to sequencing in Figure 2 are indicated by red letters and lines.

Table 1. Locus/Gene-Specific Primer Pairs: PCR Primers Used for Screening of Genomic Libraries

Locus/Gene	Primer location (forward and reverse)	Product size (bp)	Reference
CD1A (nonclassical MHC antigen gene)	F : 702 to 721 R : 888 to 907	206	Martin et al. 1987
CD1B (nonclassical MHC antigen gene)	F : 413 to 432 R : 554 to 573	161	Martin et al. 1987
CD1C (nonclassical MHC antigen gene)	F : 326 to 345 R : 529 to 548	223	Martin et al. 1987
CD1D (nonclassical MHC antigen gene	F : 2194 to 2213 R : 2328 to 2347	154	Calabi et al. 1989
CD1E (nonclassical MHC antigen gene)	F : 6815 to 6834 R : 6942 to 6961	147	Calabi et al. 1989
+P5 (a target binding site for the Wilms' tumor suppressor 1)	F : DS130694 R : RF129794	77	Nugus et al. 1996
SPTA1 (erythrocyte alpha-spectrin gene)	F : 121 to 141 R : 289 to 309	188	Linnenbach et al. 1986
MNDA (myelomonocytic specific protein)	F : 935 to 953 R : 1012 to 1031	97	Briggs et al. 1994
IFI-16 (interferon-g-induced gene)	F : 2145 to 2164 R : 2305 to 2323	179	Trapani et al. 1992
FY (Duffy blood group antigen gene)	F : 1863 to 1882 R : 2091 to 2110	248	Chaudhyri et al. 1993
FCERIA (IgE high-affinity Fc receptor)	F : 776 to 795 R : 976 to 995	220	Kochan et al. 1988
KRTC7 (EST; keratinocyte cDNA 7, probe nk686)	F : 33 to 52 R : 248 to 266	234	Konishi et al. 1993

site for the Wilms' tumor suppressor 1 gene (*WT1*), mapped previously by two-color fluorescent in situ hybridization (FISH) to 1q21–q22 (Negus et al. 1996), allowed successful amplification from the three previously mentioned YAC clones as well as a fourth one, 367B12. Three additional PAC clones (581I21, 510C21, and 681H10) were obtained by gene-walking using new primer sets corresponding to the telomeric sequence of the PAC clone 747M6 harboring the *CD1D* and *CD1A* genes (Fig. 1). The telomeric sequence of the PAC clone 510C21 contained the 5′ end region of the +P5 sequence, which therefore places this locus 200 kb centromeric to the *CD1D* gene (Fig. 1). Finally, four STS markers (D1S1600, D1S176, WI-8369, and SG4979) were in close proximity to each other, 100 kb centromeric to +P5.

Moving stepwise to the telomeric end of this segment, one BAC clone (407I14) and four PAC clones (687N3, 855N14, 987D5, and 1050C4) were isolated using PCR primers designed from the second exon of the erythrocyte alpha-spectrin (*SPTA1*) gene (Kotula et al. 1991). In addition, the nucleotide sequence at the telomeric end of a PAC clone 1050C4 revealed complete identity with 125-bp overlap to exon 36 of *SPTA1*. These results showed that *SPTA1* was located ~280 kb telomeric to the *CD1E* gene (in a telomere-to-centromere orientation) (Fig. 1). Furthermore, the myeloid cell-specific gene, *MNDA,* was mapped ~150 kb telomeric to *SPTA1* by PCR and Southern hybridization analyses of one BAC clone (407I14) using the *MNDA*-specific primer pairs and PCR products from the *MNDA* locus as a probe, respectively (data not shown). Likewise, immunologically relevant genes, the interferon γ-induced gene (*IFI-16)* (Trapani et al. 1992), and the α subunit of the IgE high-affinity Fc receptor gene (*FCERIA)* (Kochan et al. 1988) were localized ~150 kb and 450 kb telomeric to the *MNDA* gene, respectively. The Duffy blood group antigen locus (*FY*) was mapped between *IFI16* and *FCERIA*, and the keratinocyte cDNA 7 (*KRTC7*) gene (Konishi et al. 1994) was charted ~100 kb telomeric to *FCER1A* (Fig. 1). All together, we have constructed a high-resolution 1.7-Mb YAC, BAC, and PAC contig between the *+P5* and *KRTC7* loci. This contig contains at least 14 genes and *+P5*, in this (centrotelomeric) order: *+P5—CD1D—CD1A—CD1C—CD1B—CD1E—SPTA1—MNDA—IFI-16—FY—FCERIA—KRTC7* from centromere to telomere (Fig. 1). Finally, representative BACs and PACs spanning the entire contig were scanned for chimerism using FISH and fiber-FISH, which detected no such event. The same experiment confirmed the order of these clones as shown in Figure 1 (data not shown).

Genomic Sequence of the 1q21–q22 Region between the *CD1D* and *FCERIA* Genes

To establish the nucleotide sequence around the CD1 region, two BACs (456N8 and 527I23) and seven PACs (810N20, 893N23, 987D5, 713I11, 974O18, 683M11, and 622B6), which collectively span a 1.1-Mb segment between the *CD1D* and *FCER1A* genes, were subjected

to shotgun sequencing (Figs. 1, 2A). The 1,139,684 bp-long sequence (accession nos. AB045357–AB045365) was determined with a high redundancy of over 7. Overlaps between all BAC/PAC clones were ascertained at the sequence level. The overall G + C of the sequence is of 38.4%, which corresponds to the relatively A + T-rich isochore L1 (Fig. 2F; Bernardi 1995). This G + C content is, however, much lower than the densely packed 6p HLA region, which belongs to the G + C-rich isochore H1 (46.2%) (Fukagawa et al. 1995; Tenzen et al. 1997; The MHC Sequencing Consortium 1999). A closer inspection of the G + C content reveals fairly uniform dispersion throughout the entire segment, although numerous high G + C content peaks (>50%) were locally detected, and in most cases associated with expressed genes and/or CpG islands, including recognition sites for rare CG cleavage enzymes (Fig. 2E). When this 1.1-Mb region was scanned in 100-kb intervals, two 200-kb segments (the first linking the *CD1D* to *CD1E* loci and the second around the *FY* gene; physically located between 900 kb and 1,100 kb in Fig. 2A) at each end of a central 700-kb cluster were found to contain higher than average G + C contents, for instance, 40.0% and 41.3%, respectively. In contrast, the central 700-kb segment spanning nucleotide positions 200 kb to 900 kb in Figure 2A is comparatively G + C-poor, with 37.1% on average (35.8% to 38.5%) (Fig. 2F).

Analysis of the complete sequence with the `RepeatMasker2` program unveiled the following numbers of repeats: 332 *Alu*s, 191 *MIR*s, 367 *LINE*s (*LINE1*+*LINE2*), 133 *LTR*s, and 23 *MER*s. These repeats collectively occupy 47.4% of the sequence, with *Alu*s and *LINE*s representing 4.5% and 30.8% respectively, which corresponds to a density of one repeat per 3.4 kb and 3.1 kb, respectively (Fig. 2C). *LINE1* comprises 28.0% of the *LINE* sequences. A 300-kb segment between the *CD1D* and *CD1E* genes as well as a 200-kb segment around the *MNDA* gene (nucleotide positions 600–800 kb in Figure 2A) reveal high *LINE1* densities, 40.7% and 35.6%, respectively. In contrast, a 100-kb segment around the *SPTA1* gene (nucleotide position 500–600 kb in Figure 2A) displays low *LINE1* density of 11.1% (Fig. 2F). Finally, a total of 406 microsatellites, 70 di-, 79 tri-, 156 tetra-, and 101 penta-nucleotide repeats (Fig. 2D), were also identified within the sequenced 1.1-Mb region (one repeat per every 2.8 kb), very similar to the frequency observed in the HLA class I region (Shiina et al. 1999).

Gene Content

The 1.1-Mb genomic sequence stretching from *CD1D* to *FCERIA* was subjected to gene identification analysis using `BLAST, GRAIL, and Genscan`. This analysis revealed the existence of 41 genes within this segment or one gene per every 27.8 kb. These loci include two novel expressed genes (*AIM2* and *BL1A*), 10 known expressed genes (*CD1D, CD1A, CD1C, CD1B, CD1E, SPTA1, MNDA, IFI16, FY*, and *FCER1A* from centromere to telomere), 12 possibly expressed sequences (*ELL2-hom* and 11 *OR*), and finally, 17 new pseudogenes (nine *OR*, and *RPS10, KIAA0696, RB1, HMG14, kinectin, PIG8, HSPCAL1, HRAD1*) (Fig. 2B; Table 2). Focusing on the frequency of expressed genes (12), one gene per every 94.9 kb, one notes a gene density comparable to that (one gene every 70–100 kb) observed upon sequencing of the entire chromosome 21 (Ewing and Green 2000; Hattori et al. 2000) which, in turn, is almost identical to that assigned to the A + T-rich isochore L1 (Bernardi 1995). Most striking, among the 24 protein coding genes or possibly expressed sequences detected in this region, 12 are likely to fulfill immunological functions, highly redolent of the 6p-HLA region. These include *CD1D, CD1A, CD1C, CD1B, CD1E, SPTA1, MNDA, IFI-16, AIM2, FY, BL1A*, and *FCERIA* (Figs. 1, 2B).

Genomic Architecture of the CDI Region

The gene order of five *CD1* genes, was established as *CD1D—CD1A—CD1C—CD1B—CD1E* from the centromeric side, spanning ~176 kb (Fig. 2B; Table 2). The transcriptional orientation of *CD1D, CD1A, CD1C*, and *CD1E* was from centromere to telomere, whereas that of *CD1B* was the opposite. These results support those previously published by Calabi and Milstein (1986), as well as Yu and Milstein (1989). Each of the *CD1A–CD1E* loci has been known to have two alleles, designated 1 and 2 (Han et al. 1999). The exonic sequences of *CD1A–CD1E*, as established here, were in complete agreement with those from the human *CD1* cDNA sequences (GenBank accession nos. M28825, *CD1A*; M28826, *CD1B*; M28827, *CD1C*; J04142, *CD1D*; and X14975, *CD1E*) and were found to correspond to allele 1 for all these loci. Moreover, all donor/acceptor splicing sites (GT/AG) including those of *CD1E*, which has 12 alternative splicing forms (EMBL accession nos. AJ289111–AJ289122), were of canonical nature.

It has been suggested that the present-day gene organization of the *CD1* gene cluster was the result of regional duplication events from an ancestral *CD1* gene (Calabi et al. 1989; Porcelli 1995; Porcelli and Modlin 1999), as similarly predicted for the HLA class I region (Shiina et al. 1999). To detect a possible trace for such regional duplication at the nucleotide level, the 200-kb CD1 cluster was subjected to dot-matrix analysis. However, in sharp contrast to the presence of multiple reiterated building blocks with remarkable contiguous homologies in the HLA class I region (Shiina et al. 1999), no evidence for any such internal duplication events could be obtained (data not shown).

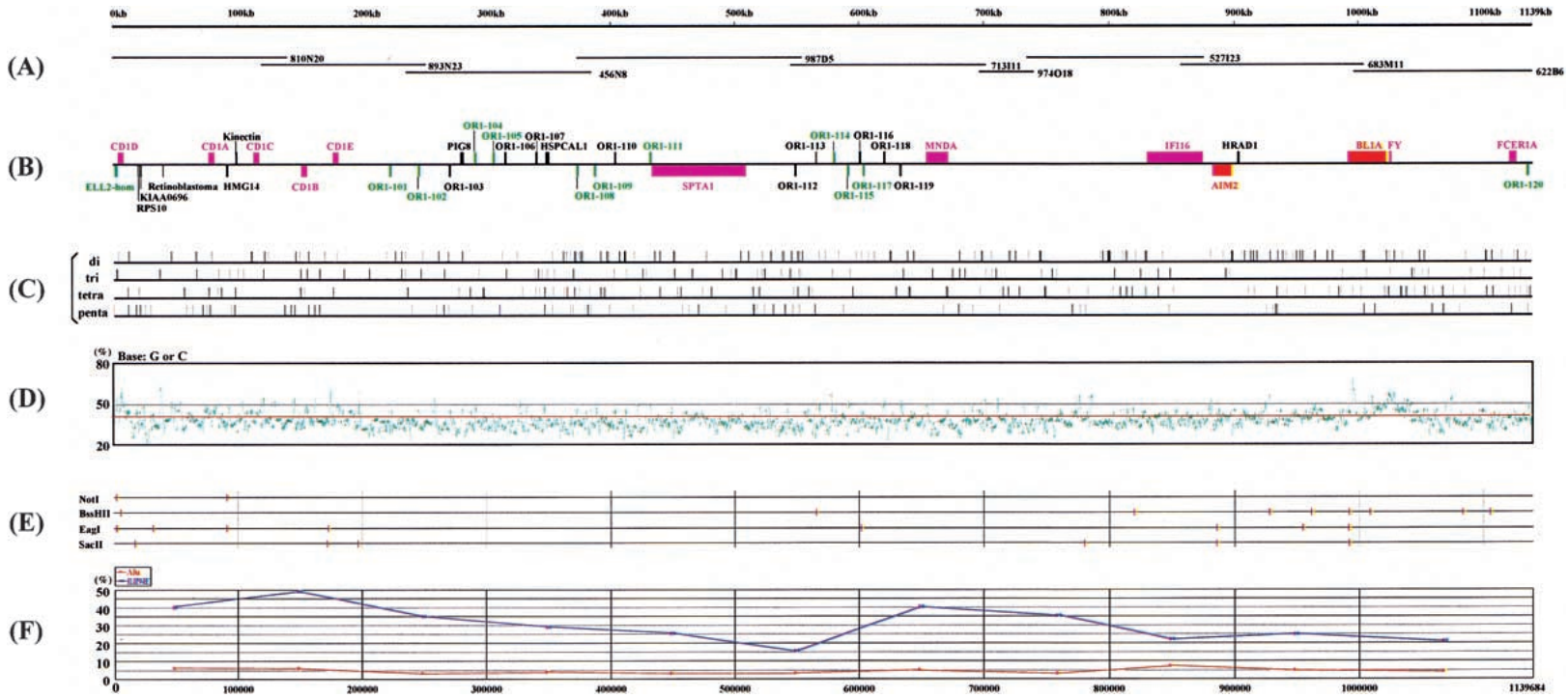

Figure 2 Structural feature of the 1.1-Mb (1,139,684 bp) region from the *CD1D* gene to the *FCER1A* gene. (*A*) An operational contig constructed by an overlapping set of two BAC (456N8 and 527I23; in boxes) and nine PAC clones (810N20, 893N23, 987D5, 713I11, 974O18, 683M11, and 622B6) was subjected to nucleotide sequencing. (*B*) Gene map. Pink boxes indicate previously mapped genes. Red boxes depict genes newly mapped in this study. Green boxes show possibly expressed sequences. Black boxes refer to pseudogenes. Upper boxes define genes oriented from centromere to telomere (from *left* to *right*), whereas lower boxes show the opposite orientation. (*C*) Location of di-, tri-, tetra-, and penta-nucleotide microsatellite repeats. (*D*) Plot of the local G + C content in overlapping 200-bp windows. A red line indicates the average G + C content (38.4%). (*E*) Recognition sites of the restriction enzymes, *Not*I, *Bss*HII, *Eag*I, and *Sac*I. (*F*) Plot of the local *Alu* and *LINE* repeat contents in overlapping 100-kb windows. Red and blue lines represent *Alu* and *LINE* repeats, respectively.

Table 2. Genes Identified around the CD1 Region

Location	Name	Orientation	Exons	Homology of prominent features
1001–2880	*ELL2*	C	1	RNA polymerase II elogation factor gene candidate, 96.3% identity with *ELL2* mRNA (U88629)
6090–10053	*CD1D*	+	6	Nonclassical HLA class Ib gene
20718–21292	*RPS10*	C	1	Ribosomal protein pseudogene, 91.1% identity with *RPS10* mRNA (U14972)
21743–22556	*KIAA0696*	C	1	Anonymous KIAA0696 pseudogene, 77.9% identity with *KIAA0696* mRNA (AB014596)
40373–40921	*RB1*	C	1	Covering the intron 17 of retinoblastoma gene, 95.7% identity with retinoblastoma gene (L11910)
79285–83389	*CD1A*	+	6	Nonclassical HLA class Ib gene
91111–92063	*HMG14*	C	1	Nonhistone chromosomal protein pseudogene, 85.0% identity with *HMG14* mRNA (J02621)
99303–99699	*Kinectin*	+	1	Human leukocyte protein pseudogene, 86.6% identity with kinectin mRNA (L25616)
114939–115270	*CD1C*	+	6	Nonclassical HLA class Ib gene
153131–156839	*CD1B*	C	6	Nonclassical HLA class Ib gene
179133–182040	*CD1E*	+	6	Nonclassical HLA class Ib gene
223667–224611	*OR1-101*	C	1	Olfactory receptor-like gene candidate
245073–246011	*OR1-101*	C	1	Olfactory receptor-like gene candidate
270215–271138	*OR1-103*	C	1	Olfactory receptor-like pseudogene
279271–281398	*PIG8*	+	1	p53-induced gene, 90.6% identity with *PIG8* mRNA (AF010313)
290707–291648	*OR1-104*	+	1	Olfactory receptor-like gene candidate
305104–306026	*OR1-105*	+	1	Olfactory receptor-like gene candidate
316364–317305	*OR1-106*	+	1	Olfactory receptor-like pseudogene
340116–341052	*OR1-107*	+	1	Olfactory receptor-like pseudogene
348757–351620	*HSPCAL1*	+	1	*HSP90* pseudogene, 90.1% identity with *HSP90* mRNA (X15183)
372273–373250	*OR1-108*	C	1	Olfactory receptor-like gene candidate
387796–388749	*OR1-109*	C	1	Olfactory receptor-like gene candidate
404157–404382	*OR1-110*	+	1	Olfactory receptor-like pseudogene
431619–432560	*OR1-111*	+	1	Olfactory receptor-like gene candidate
435886–511547	*SPTA1*	C	52	Erythrocyte alpha-spectrin gene
548931–549854	*OR1-112*	C	1	Olfactory receptor-like pseudogene
567515–567541	*OR1-113*	+	1	Olfactory receptor-like pseudogene
579716–580675	*OR1-114*	+	1	Olfactory receptor-like gene candidate
590542–591480	*OR1-115*	C	1	Olfactory receptor-like gene candidate
600096–600115	*OR1-116*	+	1	Olfactory receptor-like pseudogene
601478–602431	*OR1-117*	C	1	Olfactory receptor-like gene candidate
620848–621041	*OR1-118*	+	1	Olfactory receptor-like pseudogene
633243–634151	*OR1-119*	C	1	Olfactory receptor-like pseudogene
656196–674270	*MNDA*	+	7	Myeloid-cell-specific protein
832156–877359	*IFI16*	+	11	Interferon gamma inducible protein 16 gene
884696–899063	*AIM2*	C	6	Interferon gamma induced gene
903153–904003	*HRAD1*	C	1	Yeast RAD gene homolog, 80.6% identity with human *Rad1* -like mRNA (AF076841)
993815–1025309	*BLIA*	+	10	Cell adhesion molecule gene, similar to poliovirus receptor
1027118–1028637	*FY*	+	2	Duffy blood group antigen gene
1124517–1130405	*FCER1A*	+	5	IgE high-affinity Fc receptor gene
1134952–1136837	*OR1-120*	C	2	Olfactory receptor-like gene candidate

Location is indicated by nucleotide positions numbered from the midst of the *ELL2-hom* gene. The color code has been established as follows: Pink, known expressed genes; green, possibly expressed sequences; red, new expressed loci (i.e., for which cDNA clones were previously reported but where physical location was unknown or ambiguous); black, new pseudogenes. Gene orientation from centromere to telomere is shown by (+), whereas (C) depicts the opposite.

A Novel Cluster of Olfactory Receptor Genes

Twenty new olfactory receptor genes (*OR1-101–120* from centromere to telomere) were identified within our 1.1-Mb genomic sequence through an in silico search against various DNA databases using FASTA and BLAST (Fig. 2B; Table 2). There was no rule governing the transcriptional orientation of these olfactory receptor (*OR*) genes. The *OR1-101–119* loci were composed

of only one exon, whereas *OR1-120* consisted of two (Table 2). Nineteen (*OR1-101– -119*) of these 20 loci were clustered within a 500-kb segment between the *CD1E* and *MNDA* genes. Interestingly, this cluster is not composed solely of *OR* genes (other *OR* clusters elsewhere in the genome tend to be pure of "intruders") as it harbors three other loci, *PIG8, HSPCAL1*, and *SPTA1* (Fig. 2B). The final *OR* locus, *OR1-120*, was expelled to the end of the contig, 4.5-kb telomeric to the *FCER1A* gene. Our *OR* genes were classified into three different groups according to their structural characterization. Four loci (*OR1-110, -113, -116*, and *-118*) were classified as "fragmentary type" because of their short gene size (<300 bp), five (*OR-103, -106, -107, -112*, and *-119*) as "defective type" due to premature termination codons despite spanning a 906–939-bp stretch. Finally, the remaining 11 (*OR1-101, -102, -104, -105, -108, -109, -111, -114, -115, -117*, and *-120*) are intact, and therefore, likely to be "expressed" or "candidate" genes, despite the fact that no corresponding ESTs could be found in the current databases (this, however, might be expected, given the exquisite expression pattern of *OR* genes within the olfactory sensory neurons) (Fig. 2B; Table 2). Individual genes here are 924–975 bp in size, and carry seven transmembrane domains, common to all members of the G protein-coupled receptor (GPCR) gene superfamily (Mombaerts 1997).

To investigate the genetic relationship of these newly identified *OR* genes to other human olfactory receptor genes, a phylogenetic tree was constructed using the neighbor-joining method (Saitou and Nei 1987). The program was fed with nucleotide sequences extracted from the conserved, transmembrane segments 2–7, of all our sequences except for the fragmentary types, combined with those retrieved from 140 representative human *OR* genes deposited in GenBank and EMBL. As constructed, this phylogenetic tree allows these *OR* genes to be classified into five major families corresponding to the previously classified families (G1, G2A, G2B, G3A, and G3B) as defined by Rouquier and colleagues (1998), based on percent nucleic sequence identity (NSI) of 87 *OR* sequences (Fig. 3). All *OR* genes identified on the 1q21–q22 region belong to the G3B family indicated in blue in Figure 3. Interestingly, because *OR*s of the 1q21–q22 region except for *OR1-119* were more closely related to each other than to any other olfactory receptor genes including the 7q33–35-located *669B10.3* gene (accession no. AC004853), they may represent new subfamilies of the G3B familily. On the other hand, *OR1-119* was more closely related to the *OR* genes located on Chr.5, Chr.6, Chr.7, Chr.14, and Chr.17 than to the other *OR1* genes. More importantly, all 1q21–q22 *OR* gene family members were more closely related to their *OR* counterparts encoded within the 6p21.3–22.2 region (indicated by yellow in Fig. 3) than to the *OR* genes in other families, and the branches found in the G3B family are longer than almost *OR* genes of other families. These findings suggest that *OR* genes in the 1q21–q22 and 6p21.3–22.2 regions were created during the two rounds of duplication that generated the paralogous 1q21–q25 CD1 and 6p21.3–22.2 HLA regions (Kasahara 1999).

Other Genes

Two other novel expressed genes were identified by sequence analysis of the 1.1-Mb region. The *AIM2* gene (from nucleotide position 884696–899063) encodes an interferon-inducible protein (accession no. AF024714; DeYoung et al. 1997) and, interestingly, displays significant nucleotide homology to two neighboring centromeric genes. These are *MNDA* (from nucleotide position 656196–674270), which specifies a myeloid cell specific protein regulated by interferon α and *IFI16* (from nucleotide position 832156–877358), which encodes the interferon γ-inducible protein 16 (Table 2). Indeed, exon 5 of *AIM2* shares ~60% nucleotide identity with exon 5 of *MNDA* as well as exons 5 and 8 of the *IFI16* gene. The other novel gene identified here is *BL1A* (from nucleotide position 993815–1025309). *BL1A* encodes a cell adhesion protein (accession no. F062733) with 43% amino acid similarity to the poliovirus receptor (accession no. P32506). Two isoforms have been reported for this gene, one containing exons 1–10, whereas the other consists of exons 5, 6, 8, 9, 10, and 11 (cDNA sequences *BL1A*, accession no. F062733, and *FLJ10698*, accession no. AK001560, respectively). *SPTA1*, known as one of the causative genes of pyropoikilocytosis, encodes an erythrocyte α-specific protein (Gallagher et al. 1991). This gene spans a 75.7-kb stretch, 254-kb telomeric to the *CD1E* gene (from nucleotide position 435886–511547), with a telomere-to-centromere transcriptional orientation. The exon/intron structure determined by comparison with the *SPTA1* cDNA sequence (accession nos. J05244, M61852, and M61775–M61826; Sahr et al. 1990) was in complete agreement with that reported previously (Kotula et al. 1991). The gene is, indeed, sliced into 52 exons; all exon–intron boundaries were demarcated by canonical acceptor and donor splice sites except for the acceptor site of intron 32, which was GC instead of GT (data not shown).

DISCUSSION

To clarify the genomic structure of a critical piece of human chromosome 1q21–q22, one of four MHC-related paralogous regions, a dense 1.7-Mb YAC, BAC, and PAC contig linking the *+P5* sequence to *FCERIA* was constructed. A 1.1-Mb internal subcontig, defined by eight BAC or PAC clones harboring *CD1D* and *FCER1A* at the centromeric and telomeric ends, respectively, was subjected to DNA sequencing determina-

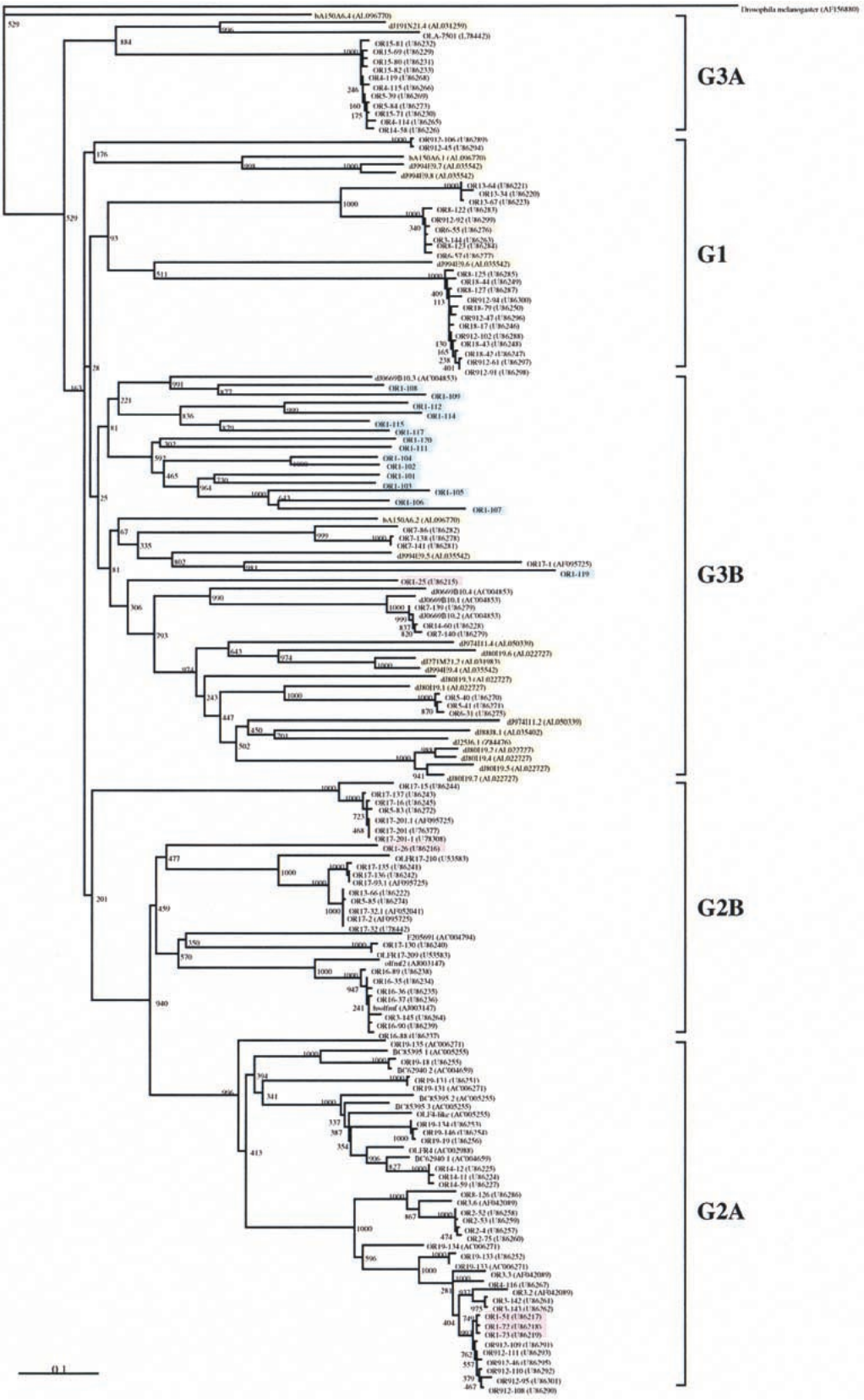

(See following page for legend.)

tion and gene mining. Among the 41 genes identified, 27 were found to have paralogous partners on the other three regions (chromosomes 6p21.3–22.2, 9q33–q34, and 19p13.1–p13.4). These were *CD1A–CD1E* at 1q21–q22—*HLA class I* at 6p21.3–22.2, 20 *OR* at 1q21–q22—21 *OR* at 6p21.3–22.2, and *SPTA1* at 1q21–q22—*SPTAN1* at 9q34.13. These facts obviously support the previous prediction that this CD1 region on chromosome 1 was created by large-scale segmental duplications along with the other three paralogous regions (Katsanis et al. 1996; Endo et al. 1997; Hughes 1998; Kasahara 1999).

The presence of an *OR* gene cluster next to the *CD1* genes, paralleling the HLA region with an *OR* gene cluster on its telomeric side (Fan et al. 1996; Ehlers et al. 2000), is intriguing. Phylogenetic tree analysis allowed clear classification of these 20 *OR* genes into only one family, G3B (Fig. 3). Most of the *OR* genes in the chromosome 1q21–q22 region were probably created during the two large-scale duplications that resulted in generation of the paralogous CD1 1q21–q25 and HLA 6p21.3–22.2 regions (Kasahara 1999) given their greater genetic relatedness to paralogues located on 6p21.3–22.2 than to *OR* genes located within other families in our phylogenetic tree (Fig. 3). Finally, because *OR* genes are conserved from *Drosophila melanogaster* to human (AF156880; Parmentier et al. 1992; Ngai et al. 1993) and distributed over multiple locations in their genomes (Rouquier et al. 1998; Trask et al. 1998), structural and comparative analyses of *OR* gene clusters from several species will make it possible to delineate the molecular dynamics of the evolutionary process through which the animal genomes evolved to the present-day complexity.

Another interesting feature of the 1.1-Mb CD1 region is that at least 23 of 37 expressed genes are immunologically relevant (Figs. 1, 2; Table 2). Again, this mirrors the HLA region, which contains at least 45 immune-affiliated genes among its 232 expressed genes (The MHC Sequencing Consortium 1999). This lends further support to the argument that the CD1 region is dedicated to the immune response, exemplified by CD1-mediated lipid or glycolipid presentation to various effector cells including γδ T, NKT, and NK cells (Porcelli and Modlin 1999) and, hence, is functionally equivalent to HLA-based peptide processing and presentation to αβ T cells (Davis and Bjorkman 1988). Based on this hypothesis, two models explaining the evolutionary generation of the MHC system can be proposed. One model is that two rounds of chromosomal duplication (chromosomes 1q21–q25, 6p21.3, 9q33–q34, and 19p13.1–p13.4) enabled two of the quadruplicate regions (chromosomes 1q21–q25 and 6p21.3) to be relaxed of functional constraints and thus allowed generation of the two major vertebrate (human) MHC systems (the CD1 and HLA-mediated antigen presentation systems). Another possibility is that the CD1 region represents the ancestral MHC system, which functioned as an "innate" immune system prior to the two rounds of chromosomal duplication (before the emergence of vertebrate). Two rounds of chromosomal duplication allowed one of the quadruplicate regions (chromosomes 6p21.3) to evolve into the HLA-mediated presentation pathway as part of the adaptive immunity system.

Dot-matrix analysis using the entire HLA class I region sequence (1.8 Mb) versus itself revealed numerous segmental duplications of a minimal building block, *MIC—HCGIX—3.8-1—P5—HCGIV—HLA class I—HCGII* (8–20 kb in size) (Shiina et al. 1999), whereas no such trace of duplication units was observed in the CD1 region. Within the *HLA* gene cluster, the occurrence of these repeated segmental duplications (which are the basis for the formation of the HLA backbone structure as well as a large variety of *HLA* class I genes) was estimated to have taken place some 20– 60 million years ago, as corroborated by dot-matrix and phylogenetic tree analyses (Shiina et al., unpubl.). Similar dot-matrix and phylogenetic analyses using *HLA* class I gene sequences as well as two mouse and one rat *CD1D* sequences (Bradbury et al. 1988; Balk et al. 1991; Ichimiya et al. 1993, 1994; Kasai et al. 1997; Matsuura et al. 1997) indicates that the origin of human *CD1* genes was some 60–100 million years ago, which places this event after the separation of mouse and human lineages (Porcelli and Modlin 1999; Shiina et al., unpubl.). Taken together, these findings suggest that the human CD1 region was established prior to the *HLA* class I region.

Of our 1.1-Mb sequence, 47% is composed of repetitive elements, among which the *LINE1* sequences occupy the largest part, 28% (Fig. 2F). This high *LINE1* density, which corresponds to that of chromosome X (26%), is twice that observed in other autosomes (on average 13%) (Lyon 1998, 2000). Although no positive or negative correlation between *LINE1* density and G + C content exists throughout chromosome X, fairly good positive correlation between *LINE1* density and G + C content has been observed in most parts of the

Figure 3 Phylogenetic tree of the olfactory receptor gene family. This phylogenetic tree was constructed employing the neighbor-joining method (Saitou and Nei 1987). Sequences were derived from the conserved region between transmembrane segments 2 and 7 in 156 olfactory receptor genes (five "defective type,", 11 "expressed gene or gene candidate type" *OR* genes in 1q21–q22 and 140 human olfactory receptor genes submitted to GenBank). Five major families classified by this phylogenetic tree were designated G1, G2A, G2B, G3A, and G3B according to Rouquier et al. (1998). Blue and yellow boxes indicate the olfactory receptor genes located on 1q21–q22 and 6p21.3, respectively. Purple and orange boxes indicate olfactory receptor genes located on chromosomes 1 and 6, respectively, but within unknown subchromosomal locations.

autosomes investigated, for example, chromosome 7 (Bailey et al. 2000). Generally, there is a positive correlation between *LINE1* and gene densities along various segments of mammalian genomes (Smit 1999; Kazazian 2000). For instance, in our own previous experiment, the entire 1.8-Mb HLA class I region could be divided into five distinct segments based on nucleotide composition; within each segment a good positive correlation between *LINE1* density and G + C content could be readily identified (Shiina et al., in prep.). In this context, it is notable that no significant positive correlation between the *LINE1* density and the G + C content was observed in the 1.1-Mb sequenced region around the CD1 region (Figs. 2D,F). In this respect, despite being an autosome, this region of chromosome 1 may be more similar to chromosome X than to other autosomes such as chromosomes 6 and 7. Although the biological significance, if any, of *LINE1* elements remains unknown, it has been suggested that on the X chromosome, they act as a "booster stations" for a heterochromatinization signal transmitted by *XIST* RNA, which in turn, leads to X chromosome inactivation (Bailey et al. 2000). Therefore, it may be possible that this CD1 region undergoes autosomal imprinting or inactivation by unknown factors such as an *XIST*-like gene.

Furthermore, it is of great interest that susceptibility loci for a number of diseases such as elliptocytosis-2, spherocytosis, pyropoikilocytosis (Gallagher et al. 1992), autosomal dominant nonsyndromic deafness, autosomal dominant nonsyndromic sensorineural 7 (Fagerheim et al. 1996), familial hemiplegic migraine (Ducrons et al. 1997), familial partial lipodystrophy (Jackson et al. 1998), and familial schizophrenia (Brzustowicz et al. 2000) were mapped to the 1q21–q23 region. This region is also known for being involved in chromosomal translocations including those in certain lymphoblastic leukemias and papillary renal cell carcinoma, for example, t (1; 19) (q23; p13) and t (X; 1) (p11; q21), respectively (Williams et al. 1984; Weterman et al. 1996). Among the genes mapped here, *SPTA1*, which encodes a erythrocyte α-spectrin, has been well established as the causative locus for the development of elliptocytosis-2, spherocytosis and pyropoikilocytosis; 23 mutations have so far been detected in these patients (http://www.ncbi.nlm.nih.gov/htbin post/Omim/dispmim? 182860). Moreover, the location of the familial schizophrenia gene was confined, by microsatellite-based mapping, to a 12-cM region on the telomeric side of +P5 (Brzustowicz et al. 2000), itself 200 kb centromeric of the *CD1D* gene. Approximately 20% of all reported cytogenetic anomalies seen in Wilms' tumor have involved chromosome 1q21–q22 (Slater and Mannens 1992). The 1.7-Mb YAC, BAC, and PAC contig around the CD1 region constructed in this study provides not only a powerful clue to dissect the binding site of several *WT1* isoforms within the +P5 region but also a blueprint to carefully analyze 1q rearrangements occurring in Wilms' tumor. Indeed, some of the newly mapped genes, including the closely packed *MNDA, IFI16* and *AIM2* , which are of potential immunological relevance, may be actually involved in the development of Wilms' tumor, or some other cancer and/or mono-polygenic/complex disorder.

In summary, we have reported the genomic cloning and sequence analysis of a prototype MHC paralogous region on human chromosome 1q. The identification of a number of immunologically relevant genes and novel olfactory receptor loci lying in close vicinity to the MHC class I *CD1* genes help to further define an emerging MHC-like functional cluster outside chromosome 6. This effort also eases positional cloning of disease-related mutations for a number of pathologies. In fine, similar high-resolution analysis on other segments of the human genome should help decipher the kinetics of vertebrate genome evolution in general.

METHODS

Construction of a YAC, BAC, and PAC Contig and Physical Mapping

Large insert yeast and bacterial clones were isolated by polymerase chain reaction (PCR)-based screening of the human CEPH (Centre d'études du Polymorphisme Humain) YAC library (Chumakov et al. 1992), a PAC library constructed from human lymphocyte DNA (Genome Systems Inc.), PAC and BAC libraries derived from human male lymphocyte DNA by Dr. Pieter J. de Jong (RPCI 4 and 5 series, and 11 series, respectively) (Osoegawa et al. 1996), and a BAC library constructed from the B cell line 978SK (Research Genetics). To construct a physical map of the 1q21–q22 region, 12 locus/gene-specific primer pairs were designed based on published sequences (Table 1), 18 STS primer pairs were selected from 70 markers positioned on the Whitehead Institute (http://carbon.wi.mit.edu: 8000/cgi-bin/contig/phys_map) WC1.16 contig map from WI-8369 (most centromeric) to UTR6608 (most telomeric), in the NCBI (http://www. ncbi. nlm.nih.gov/genemap) chromosome 1 Radiation hybrid map from D1S1600 (most centromeric) to D1S2635 (most telomeric), and 32 new STS primer sets that were prepared from 32 PAC and BAC end sequences. PCR analyses were performed using these PCR primers with YAC, PAC, and BAC DNAs as a template. PCR screening and physical mapping followed the protocol provided by Research Genetics and Osoegawa et al. (1996). Chromosomal mapping and chimerism of these BAC and PAC clones were checked by FISH, and the order of the clones within a contig was confirmed using fiberFISH as described previously (Takahashi et al. 1990, 1991; Mizuki et al. 1996; Suto et al. 1996). Southern hybridization analysis was carried out to confirm the integrity of the YAC, BAC, and PAC clones using PCR products amplified with locus/gene-specific primer pairs as probes (Inoko et al. 1986).

Sequencing Strategy

Two BACs and seven PACs covering the 1139-kb segment from the *CD1D* to *FCER1A* genes were shotgun sequenced

(Deininger 1983; Wilson et al. 1994; Rowen et al. 1996). These cloned DNAs were purified by CsCl equilibrium density gradient centrifugation. Construction of shotgun libraries and preparation of sequencing templates has been described (Mizuki et al. 1997; Shiina et al. 1998, 1999).

DNA sequencing was performed by cycle sequencing employing AmpliTaq-DNA polymerase FS (PE Applied Biosystems), fluorescently labeled dye or BigDye primers, or dye or BigDye terminators in a GeneAmp PCR system (PE Applied Biosystems). A 373S or 377 ABI PRISM DNA sequencer was used for automated fluorescent sequencing (PE Applied Biosystems).

Assembly and Database Analyses

Individual sequences were minimally edited to remove vector sequences, transferred to a SPARC station (Sun Microsystems) on the TCP/IP protocol and assembled into contigs using the GENETYX-/SQ software (Software Development Co., Tokyo). Remaining gaps or areas of ambiguity were analyzed by a direct sequencing procedure employing PCR amplification products obtained with appropriate PCR primers or by nucleotide sequence determination of shotgun clones containing the segments of interest with sequencing primers designed from the sequence data and fluorescent dideoxynucleotide chain terminators (Wilson et al. 1994).

The final sequence was initially analyzed using GENETYX software (Software Development Co.) on a Macintosh computer. Database searches (EMBL, GenBank, and DDBJ) were carried out using FASTA, BLASTN and BLASTX (Altschul et al. 1990). Because of the size limitation for sequence comparisons, dot-matrix analyses with varying parameters were used extensively to identify patterns of similarity. Searches for coding regions utilized the CRM/GRAIL, GRAIL I, GRAIL Ia, and GRAIL II gene-finding programs (http://avalon.epm.ornl.gov/Grail-1.3; Uberbacker and Mural 1991) and the GENSCAN gene-prediction program (http://gnomic.stanford.edu/~chris/GENSCANW.html), along with the SwissProt database and the Smith-Waterman algorithm. Repeat and microsatellite sequences were detected with the RepeatMasker2 (http://ftp.genome.washington.edu/cgi-bin/RepeatMasker) and sputnik programs, respectively. Prediction of the transmembrane regions of ORctory receptor-like genes was determined using the SOSUI program (http://azusa.proteome.bio.tuat.ac.jp/sosui/).

Phylogenetic Analyses

Dot-matrix analyses were performed using Harrplot 2.0 software (Software Development Co.). The phylogenetic tree was constructed employing the neighbor-joining method with sequences of the conserved region between transmembrane segments 2 and 7 of *OR* genes (Saitou and Nei 1987). Multiple alignment of sequences and calculation of genetic distance were carried out using CLUSTALW (DDBJ; http://crick.genes.nig.ac.jp/homology/clustalw.shtml).

ACKNOWLEDGMENTS

We thank Dr. Dominique Giorgi (CRBM, France) for providing us with olfactory receptor gene sequences. S.B. acknowledges support from the ACI Jeunes Chercheurs–Ministère de la Recherche and CReS-INSERM. Grants from the Japan Science and Technology Corporation (JST), an arm of the Science and Technology Agency, the Ministry of Education, Science, Sports and Culture, Japan, and the Tokai University School of Medicine supported this work.

The publication costs of this article were defrayed in part by payment of page charges. This article must therefore be hereby marked "advertisement" in accordance with 18 USC section 1734 solely to indicate this fact.

REFERENCES

Abi-Rached, L., McDermott, M.F., and Pontarotti, P. 1999. The MHC big bang. *Immunol. Rev.* **167:** 33–44.

Albertson, D.G., Fishpool, R., Sherrington, P., Nacheva, E., and Milstein, C. 1988. Sensitive and high resolution in situ hybridization to human chromosomes using biotin labeled probes: Assignment of the human thymocyte CD1 antigen genes to chromosome 1. *EMBO J.* **7:** 2801–2805.

Altschul, S.F., Gish, W., Miller, W., Myers, E.W., and Lipman, D. J. 1990. Basic local alignment search tool. *J. Mol. Biol.* **215:** 403–410.

Bailey, J.A., Carrel, L., Chakravarti, A., and Eichler, E.E. 2000. Molecular evidence for a relationship between LINE-1 elements and X chromosome inactivation: The Lyon repeat hypothesis. *Proc. Natl. Acad. Sci.* **97:** 6634–6639.

Balk, S.P., Bleicher, P.A., and Terhorst, C. 1991. Isolation and expression of cDNA encoding the murine homologues of CD1. *J. Immunol.* **146:** 768–774.

Bernardi, G. 1995. The human genome: Organization and evolutionary history. *Annu. Rev. Genet.* **29:** 443–476.

Bradbury, A., Belt, K.T., Neri, T.M., Milstein, C., and Calabi, F. 1988. Mouse CD1 is distinct from and co-exists with TL in the same thymus. *EMBO J.* **7:** 3081–3086.

Briggs, R.C., Briggs, J.A., Ozer, J., Swaly, L., Dworkin, L.L., Kingsmore, S.F., Seldin, M.F., Kaur, G.P., Athwal, R.S., and Dessypris, E.N. 1987. The Human myeloid cell nuclear differentiation antigen gene is one of at least two related interferon-inducible genes located on chromosome 1q that are expressed specifically in heamatopoietic cells. *Blood* **83:** 2153–2162.

Brzustowicz, L.M., Hodgkinson, K.A., Chow, E.W., Honer, W.G., and Bassett, A.S. 2000. Location of a major susceptibility locus for familial schizophrenia on chromosome 1q21–q22. *Science* **288:** 678–682.

Burdin, N., Brossay, L., Koezuka, Y., Smiley, S.T., Grusby, M.J., Gui, M., Taniguchi, M., Hayakawa, K., and Kronenberg, M. 1998. Selective ability of mouse CD1 to present glycolipids: Alpha-galactosylceramide specifically stimulates V alpha 14 + NK T lymphocytes. *J. Immunol.* **161:** 3271–3281.

Calabi, F. and Milstein, C. 1986. A novel family of human major histocompatibility complex-related genes not mapping to chromosome 6. *Nature* **323:** 540–543.

Calabi, F., Jarvis, J.M., Martin, L., and Milstein, C.. 1989. Two classes of CD1 genes. *Eur. J. Immunol.* **19:** 285–292.

Campbell, R.D. and Trowsdale, J. 1997. A map of the human major histocompatibility complex. *Immunol. Today* (Suppl.) **18**.

Chumakov, I.M., LeGall, I., Billault, A., Soularue, P., Guillou, S., Rigault, P., Bui, H., DeTand, M.F., Barillot, E., Abderrahim, H., et al. 1992. Isolation of chromosome 21-specific yeast artificial chromosomes from a total human genome library. *Nat. Genet.* **1:** 222–225.

Davis, M.M. and Bjorkman, P.J. 1988. T-cell antigen receptor genes and T-cell recognition. *Nature* **334:** 395–402.

Deininger, P.L. 1983. Random subcloning of sonicated DNA: Application to shotgun DNA sequence analysis. *Anal. Biochem.* **129:** 216–223.

DeYoung, K.L., Ray, M.E., Su, Y.A., Anzick, S.L., Johnstone, R.W., Trapani, J.A., Meltzer, P.S., and Trent, J.M. 1997. Cloning a novel member of the human interferon-inducible gene family associated with control of tumorigenicity in a model of human melanoma. *Oncogene* **15:** 453–457.

Ducrons, A., Joutel, A., Vahedi, K., Cecillon, M., Ferreira, A., Bernard, E., Veirer, A., Echenne, B., de Muntain, A.L., Bousser,

M.G., et al. 1997. Mapping of a second locus for familial hemiplegic migraine to 1q21–q23 and evidence of further heterogeneity. *Am. Neurol. Assoc.* **42:** 885–890.

Ehlers, A., Beck, S., Forbes, S.A., Trowsdale, J., Volz, A., Younger, R., and Zieglar, A. 2000. MHC-linked olfactory receptor loci exhibit polymorphism and contribute to extended HLA/OR-haplotypes. *Genome Res.* **10:** 1968–1978.

Endo, T., Imanishi, T., Gojobori, T., and Inoko, H. 1997. Evolutionary significance of intra-genome duplications on human chromosome. *Gene* **205:** 19–27.

Ewing, E. and Green, P. 2000. Analysis of expressed sequence tags indicates 35.000 human genes. *Nat. Genet.* **25:** 232–234.

Fagerheim, T., Nilssen, O., Raeymaekers, P., Brox, V., Moum, T., Elverland, H.H., Teig, E., Omland, H.H., Fostad, G.K., and Tranebjaerg, L. 1996. Identification of a new locus for autosomal dominant non-syndromic hearing impairment (DFNA7) in a large Norwegian family. *Hum. Mol. Genet.* **5:** 1187–1191.

Fan, W., Cai, W., Parimoo, S., Lennon, G.G., and Weissman, M. 1996. Identification of seven new human MHC class I region genes around the HLA-F locus. *Immunogenetics* **44:** 97–103.

Fukagawa, T., Sugaya, K., Matsumoto, K., Okumura, K., Ando, A., Inoko, H., and Ikemura, T. 1995. A boundary of long-range G + C% mosaic domains in the human MHC locus: Pseudoautosomal boundary-like sequence exists near the boundary. *Genomics* **25:** 184–191.

Gallagher, P.G., Tse, W.T., Coetzer, T., Lecomte, M.C., Garbarz, M., Zarkowsky, H.S., Baruchel, A., Ballas, SK., Dhermy, D., Palek, J., et al. 1992. A common type of the spectrin alpha I 46–50a-kD peptide abnormality in hereditary elliptocytosis and pyropoikilocytosis is associated with a mutation distant from the proteolytic cleavage site. Evidence for the functional importance of the triple helical model of spectrin. *J. Clin. Invest.* **89:** 892–898.

Hashimoto, K., Hirai, M., and Kurosawa, Y. 1995. A gene outside the human MHC related to classical HLA class I genes. *Science* **269:** 693–695.

Hattori, M., Fujiyama, A., Taylor, T.D., Watanabe, H., Yada, T., Park, H.S., Toyoda, A., Ishii, K., Totoki, Y., Choi, D.K., et al. 2000. The DNA sequence of human chromosome 21. The chromosome 21 mapping and sequencing consortium. *Nature* **405:** 311–319.

Han, M., Hannick, L.I., DiBrino, M., and Robinson, M.A. 1999. Polymorphism of human CD1 genes. *Tissue Antigens* **54:** 122–127.

Hughes, A.L. 1991. Evolutionary origin and diversification of the mammalian CD1 antigen genes. *Mol. Biol. Evol.* **8:** 185–201.

Hughes, A.L. 1998. Phylogenetic tests of the hypothesis of block duplication of homologous genes on human chromosomes 6, 9, and 1. *Mol. Biol. Evol.* **15:** 854–870.

Ichimiya, S., Matsuura, A., Takayama, S., and Kikuchi, K. 1993. Molecular cloning of a cDNA encoding the rat homologue of CD1. *Transplant. Proc.* **25:** 2773–2774.

Ichimiya, S., Kikuchi, K., and Matsuura, A. 1994. Structural analysis of the rat homologue of CD1. Evidence for evolutionary conservation of the CD1D class and widespread transcription by rat cells. *J. Immunol.* **153:** 1112–1123.

Inoko, H., Ando, A., Ito, M., and Tsuji, K. 1986. Southern hybridization analysis of DNA polymorphism in the HLA-D region. *Hum. Immunol.* **16:** 304–313.

Jackson, S.N., Pinkney, J., Bargiotta, A., Veal, C.D., Houlett, T.A., McNally, P.G., Corral, R., Johnson, A., and Trembath, R. 1998. A defect in the regional deposition of adipose tissue (Partial lipodystrophy) is encoded by a gene at chromosome 1q. *Am. J. Hum. Genet.* **63:** 534–540.

Kasahara, M. 1999. The chromosomal duplication model of the major histocompatibility complex. *Immnol. Rev.* **167:** 17–32.

Kasahara, M., Hayashi, M., Tanaka, K., Inoko, H., Sugaya, K., Ikemura, T., and Ishibashi, T. 1996. Chromosomal localization of the proteasome Z subunit gene reveals an ancient chromosomal duplication involving the major histocompatibility complex. *Proc. Natl. Acad. Sci.* **93:** 9096–9102.

Kasai, K., Matsuura, A., Kikuchi, K., Hashimoto, Y., and Ichimiya, S. 1997. Localization of rat CD1 transcripts and protein in rat tissues—An analysis of rat CD1 expression by in situ hybridization and immunohistochemistry *Clin. Exp. Immunol.* **109:** 317–322.

Katsanis, N., Fitzgibbon, J., and Fisher, E.M.C. 1996. Paralogy mapping: Identification of a region in the human MHC triplicated onto human chromosomes 1 and 9 allows the prediction and isolation of novel PBX and NOTCH loci. *Genomics* **35:** 101–108.

Kazazian, H.H. 2000. L1 retrotransposons shape the mammalian genome. *Science* **289:** 1152–1153.

Kochan, J., Pettine, L.F., Hakimi, J., Kishi, K., and Kinet, J.P. 1988. Isolation of the gene coding for the alpha subunit of the human high affinity IgE receptor. *Nucleic Acids Res.* **16:** 3584–3584.

Konishi, K., Morishima, Y.I., Ueda, E., Nomomura, K., Kida, S., Yamanishi, K., and Yasuno, H. 1994. Cataloging of the genes expressed in human keratinocytes: Analysis of 607 randomly isolated cDNA sequences. *Biochim. Biophys. Res. Commun.* **202:** 976–983.

Kotula, L., Laury-Kleintop, L.D., Showe, L., Sahr, K., Linnenbach, A.J., Forget, B., and Curtis, P.J. 1991. The exon-intron organization of the human erythrocyte alpha-spectrin gene. *Genomics* **9:** 131–140.

Linnenbach, A.J., Speicher, D.W., Marchesi, V.T., and Forget, B.G. 1986. Cloning a portion of the chromosomal gene for human erythrocyte alpha-spectrin by using a synthetic gene fragment. *Proc. Natl. Acad. Sci.* **83:** 2397–2401.

Lyon, M.F. 1998. X-chromosome inactivation: A repeat hypothesis. *Cytogenet. Cell Genet.* **80:** 133–137.

Lyon, M.F. 2000. LINE-1 elements and X chromosome inactivation: A function for "junk" DNA? *Proc. Natl. Acad. Sci.* **97:** 6248–6249.

Martin, L.H., Calabi, F., and Milstein, C. 1986. Isolation of CD1 genes: A family of major histocompatibility complex-related differentiation antigens. *Proc. Natl. Acad. Sci.* **83:** 9154–9158.

Martin, L.H, Calabi, F., Lefebvre, F.A., Bilsland, C.A., and Milstein, C. 1987. Structure and expression of the human thymocyte antigens CD1a, CD1b, and CD1c. *Proc. Natl. Acad. Sci.* **84:** 9189–9193.

Matsuura, A., Takayama, S., Kinebuchi, M., Hashimoto, Y., Kasai, K., Kozutsumi, D., Ichimiya, S., Honda, R., Natori, T., and Kikuchi, K. 1997. RT1.P, rat class Ib genes related to mouse TL: Evidence that CD1 molecules but not authentic TL antigens are expressed by rat thymus. *Immunogenetics* **46:** 293–306.

The MHC Sequencing Consortium. 1999. Complete sequence and gene map of a human major histocompatibility complex (MHC). *Nature* **401:** 921–923.

Mizuki, N., Kimura, M., Ohno, S., Sato, M., Ando, H., Ishihara, M., Goto, K., Ono, A., Taguchi, S., Yamazaki, M., et al. 1996. Isolation of cDNA and genomic clones of a human Ras-related GTP-binding protein gene and its chromosomal localization to the long arm of chromosome 7, 7q36. *Genomics* **34:** 114–118.

Mizuki, N., Ando, H., Kimura, M., Ohno, S., Miyata, S., Yamazaki, M., Tashiro, H., Watanabe, K., Ono, A., Taguchi, S., et al. 1997. Nucleotide sequence analysis of the HLA class I region spanning the 237 kb segment around the HLA-B and -C genes. *Genomics* **42:** 55–66.

Mombaerts, P. 1999. Seven-transmembrane proteins as odorant and chemosensory receptors. *Science* **286:** 707–711.

Negus, K., Holmes, G.H., Wicking, C., Wainwright, B.J., and Little, M.H. 1996. +P5(D1S3309E), a novel target binding site for the Wilms' tumour suppressor 1 (WT1) gene, maps to human chromosome 1q21–q22. *Cytogenet. Cell Genet.* **72:** 306–309.

Ngai, J., Chess, A., Dowling, M.M., Necles, N., Macagno, E.R., and Axel, R. 1993. Coding of olfactory information: Topography of odorant receptor expression in the catfish olfactory epithelium. *Cell* **72:** 667–680.

Osoegawa, K., Susukida, R., Okano, S., Kudoh, J., Minoshima, S., Shimizu, N., de Jong, P., Groet, J., Ives, J., Lehrach, H., et al. 1996. An integrated map with cosmid/PAC contigs of a 4-Mb down syndrome critical region. *Genomics* **32:** 375–387.

Parmentier, M., Libert, F., Schurmans, S., Schiffmann, S., Lefort, A.,

Eggerickx, D., Ledent, C., Mollereau, C., Gerard, C., Perret, J., et al. 1992. Expression of members of the putative olfactory receptor gene family in mammalian germ cells. *Nature* **355:** 453–455.

Porcelli, S. 1995. The CD1 family: A third linkage of antigen-presenting molecules. *Adv. Immunol.* **59:** 1–98.

Porcelli, S. and Modlin, R.L. 1999. The CD1 system: Antigen-presenting molecules for T cell recognition of lipids and glycolipids. *Annu. Rev. Immunol.* **17:** 297–329.

Riegert, P., Wanner, V., and Bahram, S. 1998. Genomics, isoforms, expression, and phylogeny of the MHC class I-related MR1 gene. *J. Immunol.* **161:** 4066–4077.

Rouquier, S., Taviaux, S., Trask, B.J., Brand-Arpon, V., van-den-Engh, G., Demaille, J., and Giorgi, D. 1998. Distribution of olfactory receptor genes in the human genome. *Nat. Genet.* **18:** 243–250.

Rowen, L., Koop, B., and Hood, L. 1996. The complete 685-kilobase DNA sequence of the human T cell receptor locus. *Science* **272:** 1755–1762.

Saitou, N. and Nei, M. 1987. The neighbor-joining method: A new method for reconstructing phylogenetic trees. *Mol. Biol. Evol.* **4:** 406–525.

Salter, R.M. and Mannens, M.M.A. 1992. Cytogenetics and molecular genetics of Wilms' tumor of childhood. *Cancer Genet. Cytogenet.* **61:** 111–121.

Sahr, K.E., Laurila, P., Kotula, L., Scarpa, A.L., Coupal, E., Leto, T.L., Linnenbach, A.J., Winkelmann, J.C., Speicher, W., Marchesi, V.T., et al. 1990. The complete cDNA and polypeptide sequences of human erythroid alpha-spectrin. *J. Biol. Chem.* **265:** 4434–4443.

Shiina, T., Tamiya, G., Oka, A., Yamagata, T., Yamagata, N., Kikkawa, E., Goto, K., Mizuki, N., Watanabe, K., Fukuzumi, Y., et al. 1998. Nucleotide sequencing analysis of the 146 kb segment around the IkBL and MICA genes at the centromeric end of the HLA class I region. *Genomics* **47:** 372–382.

Shiina, T., Tamiya, G., Oka, A., Takishima, N., Yamagata, T., Kikkawa, E., Iwata, K., Tomizawa, M., Okuaki, N., Kuwano, Y., et al. 1999. Molecular dynamics of MHC genesis unraveled by sequence analysis of the 1,796,938 bp HLA class I region. *Proc. Natl. Acad. Sci.* **96:** 13282–13287.

Sieling, P.A., Chatterjee, D., Porcelli, S.A., Prigozy, T.I., Mazzaccaro, R.J., Soriano, T., Bloom, B.R., Brenner, M.B., Kronenberg, M., Brennan, P.J., et al. 1995. CD1-restricted T cell recognition of microbial lipoglycan antigens *Science* **269:** 227–230.

Slater, R.M. and Mannens, M.M. 1992. Cytogenetics and molecular genetics of Wilms' tumor of childhood. *Cancer Genet. Cytogenet.* **61:** 111–121.

Smit, A.F. 1999. Interspersed repeats and other mementos of tranposable elements in mammalian genomes. *Curr. Opin. Genet. Dev.* **9:** 657–663.

Sugaya, K., Fukagawa, T., Matsumoto, K., Mita, K., Takahashi, E., Ando, A., Inoko, H., and Ikemura, T. 1994. Three genes in the human MHC class III region near the junction with the class II: Gene for receptor of advanced glycosylation end products, PBX2 homeobox gene and a Notch homolog, human counterpart of mouse mammary tumor gene int-3. *Genomics* **23:** 408–419.

Sugaya, K., Sasanuma, S., Nohata, J., Kimura, T., Fukagawa, T., Nakamura, Y., Ando, A., Inoko, H., Ikemura, T., and Mita, K. 1997. Gene organization of human NOTCH4 and (CTG)n polymorphism in this human counterpart gene of mouse proto-oncogene Int-3. *Gene* **189:** 235–244

Suto, Y., Tokunaga, K., Watanabe, Y., and Hirai, M. 1996. Visual demonstration of the organization of the human complement C4 and 21-hydroxylase genes by high-resolution fluorescence in situ hybridization. *Genomics* **33:** 321–324.

Takahashi, E., Hori, T., O'Connell, P., Leppert, M., and White, R. 1990. R-banding and nonisotopic in situ hybridization: Precise localization of the human type II collagen gene (COL2A1). *Hum. Genet.* **86:** 14–16.

Takahashi, E., Yamauchi, M., Tsuji, H., Hitomi, H., Meuth, M., and Hori, T. 1991. Chromosome mapping of the human cytidine-5′-triphosphate synthetase (CTPS) gene to band 1p34.1–p34.3 by fluorescence in situ hybridization. *Hum. Genet.* **88:** 119–121.

Tenzen, T., Yamagata, T., Fukagawa, T., Sugaya, K., Ando, A., Inoko, H., Gojobori, T., Fujiyama, A., Okumura, K., and Ikemura, T. 1997. Precise switching of DNA replication timing in the GC content transition area in the human major histocompatibility complex. *Mol. Cell. Biol.* **17:** 4043–4050.

Trapani, J.A., Brown, K.A., Dawson, M.J., Ramsay, R.G., Eddy, R.L., Show, T.B., White, P.C., and Dupont, B. 1992. A novel gene constitutively expressed in human lymphoid cells is inducible with interferon-gamma in myeloid cells. *Immunogenetics* **36:** 369–376.

Trask, B.J., Massa, H., Brand-Arpon, V., Chan, K., Friedman, C., Nguyen, O.T., Eichler, E., van-den-Engh, G., Rouquier, S., Shizuya, H., et al. 1998. Large multi-chromosomal duplications encompass many members of the olfactory receptor gene family in the human genome. *Hum. Mol. Genet.* **7:** 2007–2020.

Uberbacher, E.C. and Mural, R.J. 1991. Locating protein-coding regions in human DNA sequences by a multiple sensor-neural network approach. *Proc. Natl. Acad. Sci.* **88:** 11261–11265.

Walsh, M.T., Divane, A., and Whitehead, A.S. 1996. Fine mapping of the human pentraxin gene region on chromosome 1q23. *Immunogenetics* **44:** 62–69.

Weterman, A.J., Wilbrink, M., Dijkhuizen, T., Berg, E., and Kessel, A.G. 1996. Fine mapping of the 1q21 breakpoint of the papillary renal cell carcinoma-associated (x; 1) translocation. *Hum. Gent.* **98:** 16–21.

Williams, D.L., Look, A.T., Melvin, S.L., Roberson, P.K., Dahl, G., Flake, T., and Stass, S. 1984. New chromosomal translocations correlate with specific immunophenotypes of childhood acute lymphoblastic leukemia. *Cell* **36:** 101–109.

Wilson, R., Ainscou, R., Anderson, C.K., Baynes, C., Berks, M., Bonfield, J., Burton, J., Connell, M., Copsey, T., Cooper, J., et al. 1994. 2.2 Mb of contiguous nucleotide sequence from chromosome III of *C. elegans*. *Nature* **368:** 32–38.

Yu, C.Y. and Milstein, C. 1989. A physical map linking the five CD1 human thymocyte differentiation antigen genes. *EMBO J.* **8:** 3727–3732.

Received December 14, 2000; accepted in revised form March 6, 2001.